Available online at www.sciencedirect.com
SCIENCE DIRECT
Agricultural and Forest Meteorology 133 (2005) 140–152
AGRICULTURAL AND FOREST METEOROLOGY
www.elsevier.com/locate/agrformet

Flow divergence and density flows above and below a deciduous forest
Part I. Non-zero mean vertical wind above canopy

N.J. Froelich [a], H.P. Schmid [a,*], C.S.B. Grimmond [a], H.-B. Su [b], A.J. Oliphant [c]

[a] *Atmospheric Science Program, Department of Geography, Indiana University, 701 E. Kirkwood Avenue, Bloomington, IN 47405, USA*
[b] *East Carolina University, Greenfield, NC 27858, USA*
[c] *San Francisco State University, San Francisco, CA 94132, USA*

Received 18 April 2005; accepted 13 September 2005

Abstract

Ecosystem–atmosphere exchange flux measurements above tall vegetation in hilly terrain are well known to suffer from systematic underestimates of nighttime fluxes of CO_2 and other scalars with significant sources in or below the canopy. This bias is commonly attributed to advection driven by thermotopographic density flows and the resulting horizontal flow divergence. Flux correction methods have been proposed based on this notion. To examine the structure and dynamics of horizontal flow divergence and vertical convergence mean vertical velocities are analyzed. These are derived from sonic anemometers at 1.8 and 1.3 times canopy height for 3 years above a deciduous forest in hilly terrain at the Morgan–Monroe State Forest (Indiana, USA) Fluxnet site. Measured vertical velocities are linked to forcing parameters represented in the equations of motion and heat for sloping terrain. In the leaf-off season, the data suggest that the dynamics and daily patterns of horizontal flow divergence (implied from vertical convergence through continuity) are entirely consistent with the hypothesis that the divergence is driven by thermotopographic density flows. However, in the vegetative season with a full canopy, a more complex picture emerges, suggesting strong dynamic and thermal decoupling of the horizontal divergence below canopy from flow conditions above. Thus we conclude that flux correction methods based on above-canopy conditions alone may significantly misrepresent scalar transport below canopy during the vegetative season and should be avoided.

Keywords: Deciduous forest; Micrometeorology; Drainage flow; Advection; Vertical velocity

1. Introduction

Recent research has questioned the accuracy of eddy-covariance measurements of ecosystem–atmosphere exchange, particularly over tall vegetation in areas of complex terrain. Evidence of underestimates of nighttime respiration fluxes, during low wind conditions and low turbulence (low friction velocity), has been presented by several researchers (e.g. Wofsy et al., 1993; Black et al., 1996; Goulden et al., 1996; Jarvis et al., 1997). One potential cause of this observed underestimate is advection of mass, driven by thermotopographically driven horizontal flow divergence (drainage flows) (Goulden et al., 1996; Lee, 1998). A simplified analytical model to correct for this advection loss, by linking measured vertical flow convergence above the canopy to horizontal divergence, has been

* Corresponding author. Tel.: +1 812 855 6125; fax: +1 812 855 1661.
E-mail address: hschmid@indiana.edu (H.P. Schmid).

0168-1923/$ – see front matter © 2005 Elsevier B.V. All rights reserved.
doi:10.1016/j.agrformet.2005.09.005

proposed by Lee (1998) and was found to be effective at some sites (Lee and Hu, 2002; Aubinet et al., 2003); however, others (Finnigan, 1999; Baldocchi et al., 2000) question whether this approach is generally applicable, in complex three-dimensional flows.

Here, we examine flow above Morgan–Monroe State Forest (MMSF), a site located in complex topography (Schmid et al., 2000), for evidence of vertical flow convergence, and for indications that this divergence may be associated with thermotopographic flow.

2. Methods and materials

2.1. Site and instrumentation

Measurements used in this study were made on a micrometeorological tower at the MMSF AmeriFlux site (south-central Indiana, USA, 39°19′N, 86°25′W, with the base of the tower at an elevation of 280 m.a.s.l), between January 1999 and December 2001. The site is in a secondary successional mixed deciduous forest with a mean canopy height of about 25–27 m and dominant trees 60–80 years old (Ehman et al., 2002). The vegetation area index (VAI) varies from 1.0 (leaf-off) to a peak of approximately 4.5 based on LI-2000 measurements (LI-COR, Lincoln, NE). The tower is located such that the fetch of essentially uninterrupted forest is greater than 4 km in any direction and is 8 km in the prevailing wind direction (westerly to south-westerly) (Schmid et al., 2000).

The area is dominated by ridge-ravine topography with relative relief less than 60 m over length-scales of several hundred meters (Fig. 1; Schmid et al., 2000). The tower is located on Orcutt Ridge, which extends in a northwesterly–southeasterly direction. The terrain slopes downward to the southwest and northeast, with two ravines cut into these slopes; each ravine is oriented approximately radially to the tower and has an elevation drop of approximately 80 m over a distance of 2–3 km.

The MMSF tower is 46 m tall (about 1.76 times canopy height), and is instrumented to measure eddy covariance fluxes at three heights, as well as a four component radiation balance and vertical profiles of temperature, relative humidity, photosynthetically active radiation (PAR), and CO_2 and H_2O concentrations. Detailed descriptions of the tower structure,

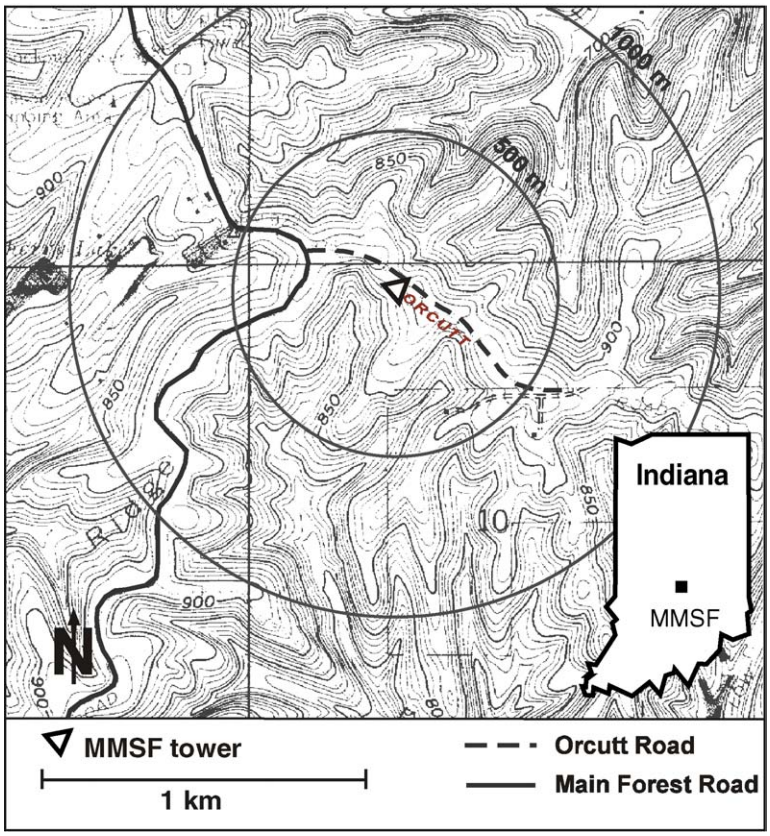

Fig. 1. Map of MMSF AmeriFlux site. Contours based on USGS map. Contour interval: 10 ft (3.05 m).

instrumentation, data collection, and data processing are given in Schmid et al. (2000).

For this study, wind velocity vectors and sonic temperatures were measured at 46 and 34 m using three-dimensional sonic anemometers (CSAT, Campbell Scientific Inc. (CSI), Logan, UT); these anemometers were positioned on beams extending to the southwest of the tower. The four components of the radiation balance (incoming and outgoing, shortwave and longwave radiation; measured with CNR1, Kipp and Zonen, Bohemia, NY) measured at two heights (46 and 34 m) were also used. Data were sampled at 10 Hz and processed to determine both 15 min and hourly mean values (Schmid et al., 2000).

It may be expected that flow patterns in and above the forest canopy will change with the amount of leaf coverage. To address this, ''seasons'' were defined by analysis of vegetation area index (VAI), measured approximately once a week with the LI-2000 system, and through photographs taken from both above and below the forest canopy. The leaf-off season includes days with no leaf coverage and bare branch canopy (VAI $\approx$ 1.0); during these periods, flow is likely affected by the topography of the ground. During the leaf-on season, there is a closed canopy (peak VAI $\approx$ 4.5) and flow patterns are likely also affected by the presence of the canopy and the ''topography'' of its top. Start and end dates of each season are listed in Table 1.

2.2. Method for calculating vertical velocities

It is expected that mean vertical flow velocities (over time-scales of 15 min to several hours) occurring over the forest canopy at MMSF will be small (on the order of 0.1 m s^{-1}) (Lee, 1998; Baldocchi et al., 2000; Paw U et al., 2000; Su et al., 2000). These vertical velocities are difficult to quantify because of uncertainties in defining the orientation of the vertical-axis. Choice of coordinate system is critical because vertical velocities are small compared to horizontal velocities; as a result, a small amount of offset in the choice of coordinate system leads to large apparent vertical velocities with large errors (Lee, 1998). In general, one may not simply use the vertical velocity measured in the sensor coordinate system, because it is likely not oriented to ''true vertical'', which in itself is not uniquely defined. It has become common practice (Smith et al., 1985; McMillen, 1988) to rotate wind vectors to a coordinate system in which the mean vertical velocity, over the Reynold's averaging period, is zero; such a coordinate system is assumed to be oriented to the mean streamline of flow over the terrain. However, if it is suspected that vertical advection is occurring, driven by small mean vertical velocities, then this approach is not valid and the coordinate system may not be oriented to the long-term streamlines. It has been suggested that it would be more appropriate to choose a ''long-term flow'' coordinate system in which the mean vertical velocity is zero over a much longer averaging period (at least several weeks). Such a coordinate system may better approximate the mean streamline of flow over the terrain and allows for non-zero mean vertical velocities over time-scales up to several hours or days (Lee, 1998; Baldocchi et al., 2000). Several methods have been proposed to transform velocity vectors, measured in the instrument coordinate system, to this long-term coordinate system: a linear regression method (Lee, 1998); a coordinate rotation (Finnigan et al., 2003); and the planar fit method (Wilczak et al., 2001).

Table 1
Start and end dates of ''seasons'', based on amount of leaf coverage

Year	Season	Start date	End date	DOY
1999	Leaf-off	January 1	March 19	1–78
	Spring transition	March 20	May 4	79–124
	Leaf-on	May 5	October 7	125–280
	Fall transition	October 8	November 24	281–328
1999–2000	Leaf-off	November 25, 1999	April 6, 2000	329–97
2000	Spring transition	April 7	May 9	98–130
	Leaf-on	May 10	October 11	131–285
	Fall transition	October 12	November 8	286–313
2000–2001	Leaf-off	November 9, 2000	April 5, 2001	314–95
2001	Spring transition	April 6	May 9	96–129
	Leaf-on	May 10	September 28	130–271
	Fall transition	September 29	October 26	272–299
	Leaf-off	October 27	December 31	300–365

Leaf-on was defined as approximately full leaf coverage, leaf-off as no leaf coverage, and spring and fall as the transition periods.

Lee (1998) used a linear regression to determine the "true" mean (hourly) vertical velocity, $\bar{w}$, as:

$$\bar{w} = \hat{w} - a(\varphi_i) - b(\varphi_i)\hat{u} \quad (1)$$

where a and b are coefficients determined, for each azimuthal bin φ_i, by a linear regression of $\hat{w}$ on $\hat{u}$, the measured mean (hourly) vertical and horizontal velocities in the instrument coordinate system. This method may be considered as the removal of an offset, $a(\varphi)$, in measured vertical velocity, followed by a rotation through an angle $\tan^{-1} b(\varphi)$. The offset may result from deflection of flow by the sensor or the supporting tower or from non-zero offsets in instrument electronics. However, because this method is based on an ordinary least squares regression, it will eliminate all linear dependence (i.e. all correlation) of $\bar{w}$ on $\hat{u}$; this method will have the apparent, but not necessarily valid, result (if all data are used in the regression) that vertical motions occur nearly uniformly during all wind conditions and are not driven by some phenomenon that is inhibited or enhanced by high or low winds.

Alternately, the mean vertical velocity may be determined by rotating from the sensor coordinate system to the apparent streamline coordinate system:

$$\bar{w} = -\hat{u}\sin\alpha(\varphi) + \hat{w}\cos\alpha(\varphi). \quad (2)$$

The vertical rotation angle, α, is determined for each azimuthal bin, φ_i, from the long-term means of the velocity components:

$$\tan\alpha(\varphi_i) = \frac{\sum_{\varphi_i}\hat{w}}{\sum_{\varphi_i}\hat{u}}. \quad (3)$$

The rotation method does not explicitly account for an offset; however the calculated rotation angle will be influenced by any offset.

With the planar fit method (Wilczak et al., 2001), all velocity vectors are transformed to a coordinate system in which "vertical" is chosen as the direction normal to a best-fit plane through all velocity vectors. This method is most appropriate for terrain that approximates a plane. In the modified planar fit method, data are divided into several azimuthal bins, corresponding to piece-wise planar topography, with different best-fit planes calculated and applied to each bin. Because the topography at MMSF is quite complex and only approximates planes in narrow azimuthal bins, this method will not be used here.

It should be noted that if there is a bias at a given site to one direction of motion (e.g. if there is a tendency to downward flow at night, but no preferred direction of motion during the day), then either of these transformation methods may produce a systematic offset in the vertical velocity (Lee, 1998); nevertheless, since the intent here is only to examine patterns and trends in the vertical motion and relations to potential driving forces, and not to use these vertical velocities to correct for advection, such an offset is not important here.

Mean vertical velocities were calculated for each 1 h interval, by coordinate rotation and by the linear regression method, using rotation angles and regression coordinates determined for each 10° wind direction bin. It was found that for each individual hourly time period slightly different vertical velocities were calculated by the two methods; however, the difference between the two methods was less than 0.02 m s^{-1} for more than 85% of the data. The choice of method for coordinate transformation could have a significant impact when vertical velocities are used to correct measured fluxes (e.g. Su et al., 2004) and should be considered more carefully in such corrections. However, the analyses discussed in Sections 3.2 and 3.3 were originally made using both methods and no noticeable difference was found in observed statistical trends and relations between these two methods. Therefore, for the remainder of the paper, analyses of vertical velocities determined using only the coordinate rotation method will be discussed.

3. Results

3.1. Rotation angles

Mean rotation angles were calculated for each 10° wind direction bin, using only velocity vectors with magnitude greater than 0.5 m s^{-1}; this lower limit on velocities used in determining the coordinate transformation was chosen because it is believed that the problem of horizontal flow divergence is worse at low wind speeds (Black et al., 1996; Goulden et al., 1996). The observed vertical rotation angle ($\tan^{-1}\hat{w}/\hat{u}$) for each hourly period and the mean vertical rotation angle (α) for each 10° azimuth bin are both shown, as a function of wind direction, in Fig. 2. The mean rotation angle (Figs. 2 and 3a) may be compared with the local topography (see Figs. 1 and 3b). The rotation angle is largest when the wind is from the northeast (10–70°) or southwest (200–260°), directions from which the wind blows up slopes and gullies. The rotation angle is near zero when the wind is from the southeast or northwest, the directions in which the terrain is relatively flat along Orcutt Ridge. The mean rotation angles are of smaller magnitude than the slope angles (Fig. 3), as expected, because streamlines at height are generally less steep than those at the surface (e.g. Finnigan and Brunet,

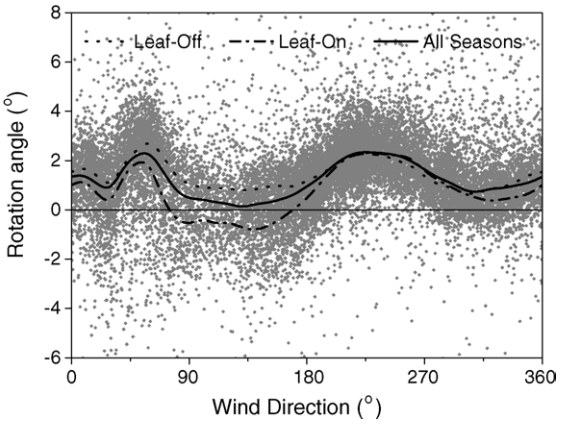

Fig. 2. The relation between vertical rotation angle at 46 m and wind direction: the observed hourly rotation angle ($\hat{w}/\hat{u}$) (data points), the mean rotation angles (α) during leaf-off (dotted line), leaf-on (dot-dash line), and all seasons combined (solid line). All data from 1999 to 2001 with horizontal velocities $\hat{u} > 0.5\,\mathrm{m\,s^{-1}}$ are included. Flow from the northeast (30–70°) may have been distorted by the tower and the body of the sonic anemometer.

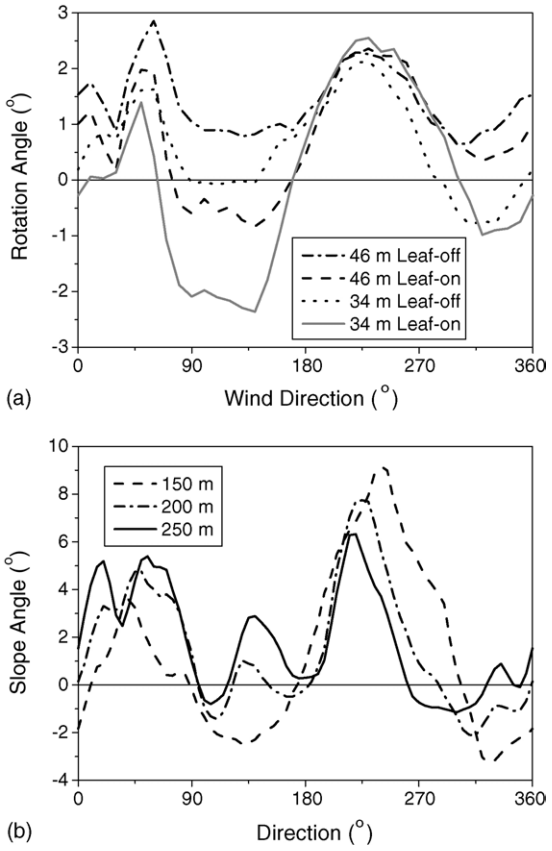

Fig. 3. (a) The mean vertical rotation angle (α) at 46 and 34 m, during leaf-off and leaf-on. This is influenced by the terrain slope. (b) The average terrain slope was determined from the ratio of the change in elevation to distance from a point to the tower. This is shown for points at distances of 150 m (dashed line), 200 m (dot-dash line) and 250 m (solid line).

1995). The maxima and minima of the slope angles and rotation angles are not perfectly aligned; however this should not be expected in the complex topography of this site.

The rotation angles were different at 34 m from those at 46 m (Fig. 3a). It has been observed that in flow over an isolated hill or ridge, the flow closer to the surface is deflected more by the topography and has steeper streamlines than flow higher up (e.g. Finnigan and Brunet, 1995). Consequently, one might expect that vertical rotation angles observed in flow over a ridge-top would be closer to zero with increasing height. This is the opposite of what is seen at MMSF: vertical rotation angles are more positive at 46 m than at 34 m, particularly in easterly and northwesterly directions. This likely occurs because the 34 m sensor is embedded in streamlines influenced by the more gradual slopes near the ridge-top at shorter distances (~100–200 m); at 46 m, the flow is likely influenced more by steeper topography dropping off into the gullies at slightly larger distances (Fig. 3b). In addition, as the 46 m sensor is located at the tower top, some vertical deflection of the flow over the obstacle of the tower may contribute to the more positive mean rotation angles, whereas the 34 m sensor is likely mostly influenced by horizontal deflection around the tower and less by vertical deflection. The rotation angle for the 46 m sensor is much less positive from azimuth angles of 10–40° than in surrounding directions, corresponding to the effect of a ridge apparent in the average slope angle of the topography at the larger distances (~250–600 m). This decrease in rotation angle at this azimuth range at 46 m may also be influenced by flow distortion by the tower.

It might be expected that flow patterns above canopy change with canopy cover. This was observed: mean rotation angles were generally lower in leaf-on, as compared to leaf-off, particularly in northerly, easterly and southerly directions (Fig. 3a). Within each season, however, rotation angles were consistent (not shown). The leaf-off rotation angles reflect response of the flow to the topography of the ground, while the leaf-on rotation angles likely are influenced both by the ground and by the canopy top. The presence of the canopy contributes to the differences between the seasons in two ways. The topography of the canopy top appears less steep than the ground topography, since trees are generally taller in the gullies than on the ridge-top. Secondly, with the canopy ‘‘surface’’ closer to the

sensor than ground, the sensor will be affected by the more gradual topographic slope angles closer to the tower. Because of these consistent differences in rotation angles between seasons, long-term rotation angles were estimated and applied to calculate vertical velocities, for each season. Rotation angles and calculated vertical velocities are likely less accurate for the spring and fall transition periods than for fully leaf-on and leaf-off, because of the changing canopy conditions and the resulting change in flow streamlines and estimated rotation angles. Moreover, these transition seasons are shorter, and have fewer data points and thus higher standard errors in estimates. For these reasons, analysis of vertical velocities focuses on the fully leaf-off and leaf-on periods.

3.2. Variability of vertical velocities

Mean vertical velocities (for each 10° wind direction bin, season and measurement level, for both 15 min and hourly averaging periods) were analyzed for statistical trends in temporal and spatial variability and for relations with other atmospheric parameters, which may be related to the processes driving the vertical motion.

3.2.1. Variability of vertical velocities with height

Vertical velocities at 34 and 46 m are generally coherent; when vertical velocities at 46 m are upward (downward), the corresponding velocities at 34 m tend to be in the same direction (Fig. 4; $R^2 = 0.56$). The vertical velocities at 34 m are generally lower than those at 46 m. An interpretation of the regression slope between vertical velocities at the two heights is offered by considering the continuity equation:

$$\frac{\partial w}{\partial z} = -\frac{\partial u}{\partial x} - \frac{\partial v}{\partial y} = -\nabla_h \cdot \mathbf{u} \tag{4}$$

where (u, v, w) are components of the wind velocity vector in the (x, y, z) directions. The vertical convergence $(-\partial w/\partial z)$ is equal to the horizontal divergence $(\nabla_h \cdot \mathbf{u})$ of the (horizontal) velocity. The vertical velocity at each height may be determined by integrating with respect to height, yielding a ratio of the vertical velocities at 34 and 46 m:

$$\frac{w_{34}}{w_{46}} = \frac{\int_0^{34} (\nabla_h \cdot \mathbf{u})\, dz}{\int_{34}^{46} (\nabla_h \cdot \mathbf{u})\, dz + \int_0^{34} (\nabla_h \cdot \mathbf{u})\, dz} = \frac{34\langle \nabla_h \cdot \mathbf{u} \rangle_{34-0}}{12\langle \nabla_h \cdot \mathbf{u} \rangle_{46-34} + 34\langle \nabla_h \cdot \mathbf{u} \rangle_{34-0}} \tag{5}$$

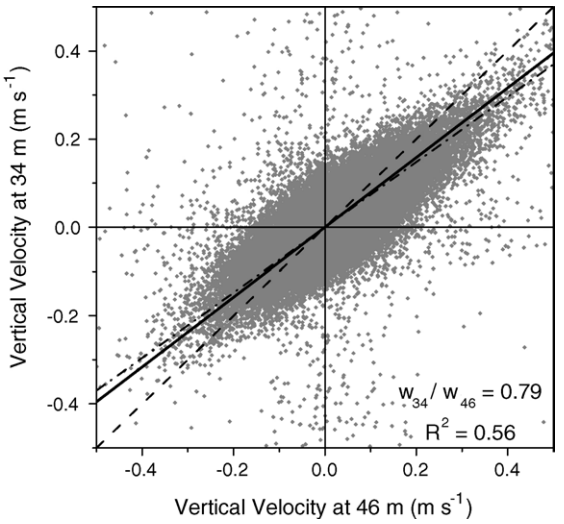

Fig. 4. Comparison of the (corrected) mean vertical velocities at 34 and 46 m. The slope of a principal-axis regression of these data (0.79; solid line) is larger than the ratio of the two heights (34/46 = 0.74; dot-dash line) and smaller than a 1:1 relation (dashed line). 15 min data from 1999 to 2001 are shown.

where $(\nabla_h \cdot \mathbf{u})_{b-a} = \frac{1}{b-a}\int_a^b (\nabla_h \cdot \mathbf{u})\, dz$ is the average horizontal divergence in a layer from a to b. A regression slope of $w_{34}/w_{46} = 1$ would indicate that there is no mean horizontal divergence between 34 and 46 m, while a slope of zero would indicate no mean horizontal divergence at heights less than 34 m. Horizontal divergence that is uniform with height would result in a ratio of vertical velocities equal to the ratio of the two heights: $w_{34}/w_{46} = 34/46 = 0.74$. A slope less (greater) than 0.74 would indicate divergence that is weaker (stronger), on average, below 34 m than between 34 and 46 m.

The slope of a principal-axis regression (Mark and Church, 1977) of vertical velocities at the two heights $(w_{34}/w_{46} = 0.79)$ is smaller than 1, but is larger than the ratio of the two heights (0.74) or the ratio of the heights above the displacement height $((34 - d)/(46 - d) = 0.55$; $d = 0.75\,h$, where h is the canopy height; $h = 26$ m). This suggests that the vertical motion is driven by a horizontal convergence/divergence that is, on average, 1.3 times stronger below 34 m than between 34 and 46 m (Table 2). This lends support to the notion that vertical velocities are driven by processes occurring at or near the surface, rather than by a synoptic-scale subsidence. However, this is in contrast with the assumption of vertically uniform convergence/divergence that is used in Lee's (1998) correction for vertical advection.

The relation between 34 and 46 m vertical velocities changes with season. The slopes of the principal-axis

Table 2
Relation between 15 min mean vertical velocities at 34 and 46 m for each season

Season	Year	Number of samples	R^2	P.A. slope	Intercept (m s^{-1})	γ
Leaf-off	1999	4929	0.619	0.804	−0.0012	0.691
	1999–2000	9882	0.556	0.822	0.0044	0.613
	2000–2001	8265	0.653	0.777	0.0060	0.815
	2001	5266	0.690	0.862	0.0057	0.453
Leaf-on	1999	8733	0.593	0.795	0.0015	0.729
	2000	10986	0.352	0.733	0.0011	1.031
	2001	11331	0.476	0.724	0.0032	1.082
All data	1999–2001	73982	0.559	0.790	−0.0012	0.754

The slope and intercept are of principal-axis (P.A.) regression line with equation: $w_{34} = \text{slope} \times w_{46} + \text{intercept}$. The ratio of the average horizontal divergence between 34 and 46 m to the average horizontal divergence below 34 m ($\gamma = \langle \nabla_h \cdot \mathbf{u} \rangle_{46-34} / \langle \nabla_h \cdot \mathbf{u} \rangle_{34-0}$) was calculated using Eq. (5).

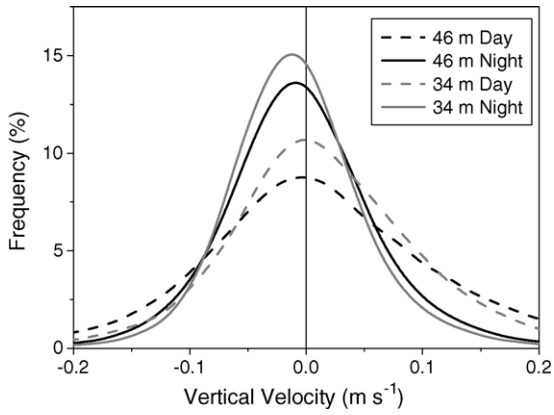

Fig. 5. Frequency distribution of corrected 15 min mean vertical velocities, for daytime and nighttime periods. Histogram bins were each of size 0.02 m s^{-1}. Sample sizes were: 46 m day, 36,291; 46 m night, 35,832; 34 m day, 37,207; 34 m night, 37,602.

regressions are generally higher in leaf-off than in leaf-on (Table 2). While these slope estimates are subject to large error due to the low correlation/large scatter, this seasonal difference in slope may be indicative of a seasonal change in flow pattern. During leaf-off, the regression slopes are between 0.74 and 1, indicating divergence driven by processes occurring at or near the surface. However, during the leaf-on seasons in both 2000 and 2001, the relation between 34 and 46 m vertical velocities had a slope less than 0.74—i.e. vertical convergence or divergence was stronger, on average, at heights between 34 and 46 m than at heights below 34 m. One possible way for this pattern to occur is with convergence/divergence that is approximately uniform above the canopy "surface" and much weaker or reversed below canopy. This hypothesis is supported by evidence of leaf-on nighttime horizontal flow convergence below canopy (Froelich and Schmid, 2002), which will be discussed in detail in Froelich and Schmid (2005). The correlation between 34 and 46 m vertical velocity is also lower in leaf-on, suggesting that the presence of a thick leaf canopy may result in more complex flow patterns and stronger decoupling between the flow above and below canopy.

3.2.2. Temporal variability in vertical velocities

Daytime and nighttime distributions of vertical velocities at each height show a tendency to more downward motion at night than during the day (Fig. 5). There is not enough evidence in the data to suggest whether this tendency is stronger at one measurement height or the other, or stronger in one season or the other.

Vertical motion is not uniform throughout the day or night. The mean, standard error of the mean, and standard deviation of vertical velocity and the frequency of upward and downward vertical velocities were calculated for each hour of the day (Fig. 6). In this ensemble average, vertical velocity was most positive during mid-day (10:00–17:00), near zero in the evening, gradually decreased after midnight, and was most negative shortly before sunrise. The calculated standard errors of the mean suggest that the mean of the vertical

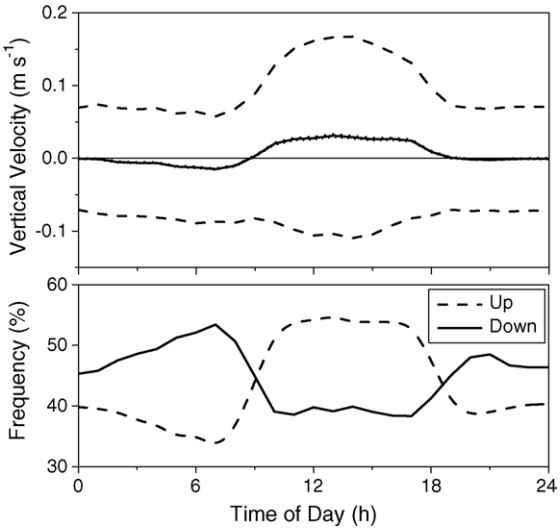

Fig. 6. Daily variability in mean vertical velocities, at 46 m (calculated from 15 min mean vertical velocities, 1999–2001). Upper panel: solid line is the mean of the vertical velocities during each hourly interval; dotted lines are ±1 standard deviation from the mean; small hashes on the solid line show the standard error of the mean. Lower panel: frequency of occurrence of downward (solid line) and upward (dashed line) velocities ($|w| > 0.005$ m s^{-1}).

velocities was positive during daytime and negative at night; however, they are not rigorously determined as they are based on time series of data with some autocorrelation. In addition, there was a higher probability of occurrence of upward motion during mid-day and of downward motion shortly before sunrise. This pattern was noted in each season (not shown), with the timing of the transitions between negative and positive mean vertical velocities shifting slightly, as might be expected, with the timing of sunrise and sunset. In both seasons, the variance in vertical velocities was larger during daytime than at nighttime; this is likely due to convection.

It should be stressed again that these are not absolute measures of vertical motion, since they were calculated under the assumption that there is not a preferred direction of vertical motion at the site. There is a tendency, however, to downward motion during nighttime hours, relative to daytime.

3.3. Relations with forcings

The vertical velocities observed indicate nocturnal vertical flow convergence and, given continuity (4), horizontal flow divergence. We suspect that horizontal divergence may be associated with downslope thermotopographic flows. While the topography at MMSF is quite complex, it is instructive to consider the drivers of a thermotopographic flow on a simple slope with angle, α, as described by momentum equations. We use the Boussinesq approximation, expressed here in a natural coordinate system (following, e.g. Whiteman, 1990), with mean velocity components $\tilde{u}$ and $\tilde{w}$ oriented in the along slope (s, increasing downslope) and slope-normal (n, increasing upward) directions:

$$\begin{aligned}
&\frac{\partial \tilde{u}}{\partial t} + \tilde{u}\frac{\partial \tilde{u}}{\partial s} + \tilde{w}\frac{\partial \tilde{u}}{\partial n} \\
&\quad = -\frac{1}{\rho_0}\frac{\partial (p - p_0)}{\partial s} - g\frac{\theta - \theta_0}{\theta_0}\sin\alpha - \frac{\partial \overline{\tilde{u}'\tilde{w}'}}{\partial n}, \\
&\frac{\partial \tilde{w}}{\partial t} + \tilde{u}\frac{\partial \tilde{w}}{\partial s} + \tilde{w}\frac{\partial \tilde{w}}{\partial n} \\
&\quad = -\frac{1}{\rho_0}\frac{\partial (p - p_0)}{\partial n} + g\frac{\theta - \theta_0}{\theta_0}\cos\alpha \approx 0
\end{aligned} \tag{6}$$

Here, θ represents the potential temperature, ρ is the density of air, and p is the pressure; terms with subscript "0" denote the mean conditions in the absence of slope flow, unsubscripted terms denote locally perturbed mean conditions associated with cooling/warming within the slope flow layer, and primed terms denote turbulent fluctuations from the ensemble. It is assumed that the ambient air, in the absence of thermotopographic flow, is at rest. In this framework, along-slope motion is governed by the pressure gradient and buoyancy associated with cooling in the slope flow layer, and turbulent stress. For small-scale flows (as at MMSF), the Coriolis force is generally neglected. The rate of heating or cooling, described by the conservation equation for heat (following Whiteman, 1990):

$$\frac{\partial \theta}{\partial t} + \tilde{u}\frac{\partial \theta}{\partial s} + \tilde{w}\frac{\partial \theta}{\partial n} = -\left[\frac{1}{\rho_0 c_\mathrm{p}}\frac{\partial Q^*}{\partial n}\right] - \left[\frac{\partial \overline{\tilde{w}'\theta'}}{\partial n}\right] \tag{7}$$

is driven by divergence of the radiation flux, Q^*, and of the (kinematic) sensible heat flux, $\overline{\tilde{w}'\theta'}$. Here, c_p, represents the specific heat. Latent heat flux divergence is often ignored.

The hypothesis that vertical velocities are driven by thermotopographic flows can be examined by relating vertical velocities to atmospheric parameters that are associated with terms in the governing equations of thermal flows, (6) and (7). Pressure gradient data over the required small spatial scales are not available at this site, and estimates of the turbulent fluxes ($\overline{\tilde{w}'\theta'}$ and $\overline{\tilde{u}'\tilde{w}'}$) are not independent of the method used for determining mean vertical velocities; however, the role of buoyancy may be examined via temperature gradient and radiative loss. In addition, relations of vertical velocity with friction velocity and stability are also considered, as strong wind shear and turbulent mixing may weaken a temperature inversion, thereby inhibiting, weakening, or dissipating thermotopographic flows.

Vertical velocities are likely influenced by numerous factors, some random and some deterministic, and many of them unknown. As a result there is generally large scatter in the relation between velocity and any given controlling parameter. This scatter represents the residual variability due to the ensemble of unaccounted factors and their interactions, and random uncertainties. Comparisons of individual independent variables to velocity are made, here, using bin-averaging to reduce random scatter and, ideally, to simulate holding all other deterministic parameters constant. Hourly averages of vertical velocities and possible deterministic forcings were used, because there may not be an instantaneous response to individual forcings; use of hourly data may help to reduce the amount of random influence on vertical velocities. We show vertical velocities in units

of cm s^{-1} (1 cm s^{-1} = 0.01 m s^{-1}) to make values more tractable.

3.3.1. Temperature gradient and buoyancy

In theoretical discussions and modeling studies, buoyancy is related to the fractional difference between the actual temperature in the thermotopographic flow layer and the ambient temperature of that layer in the absence of cooling or heating. In practice, this ambient temperature cannot be known. However, if we assume that there is neutral potential temperature stratification in the absence of cooling-driven thermotopographic flow, the potential temperature aloft may approximate the ambient potential temperature that would occur in the absence of cooling. In other observational studies of thermotopographic flows, a change in temperature with height within some portion of the slope flow layer is frequently used to indicate buoyancy (e.g. Clements et al., 1989; Doran et al., 1990; Sakiyama, 1990; Amanatidis et al., 1992); a positive (negative) vertical temperature gradient is indicative of cooling (warming) in the thermotopographic flow layer and a downward (upward) buoyancy force. Here, we use the temperatures as measured by the sonic anemometers at 46 and 34 m to estimate the mean temperature gradients.

In Fig. 7, hourly vertical velocity data were binned according to the mean temperature gradient between 46 and 34 m. At both 46 and 34 m, the mean vertical velocity decreases and the probability of downward vertical velocities increases with increasing temperature gradient (strengthening temperature inversion). This is consistent with the theory that vertical convergence above canopy may be driven by nocturnal thermotopographic downslope flows.

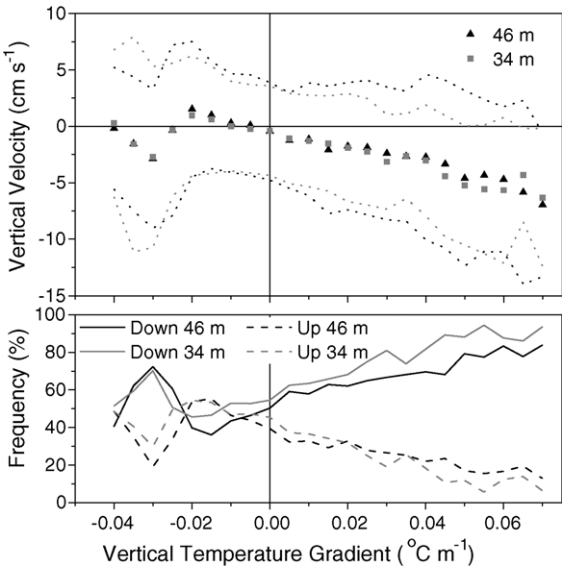

Fig. 7. Nighttime variation of hourly mean vertical velocity with temperature gradient (bin-averaged). Temperature gradients were calculated using sonic virtual temperatures at 46 and 34 m. Upper panel: mean vertical velocity in each bin at 46 (black ▲) and 34 m (gray ■); dotted lines represent ±1 standard deviation from the mean. Lower panel: frequency of occurrence of downward (solid lines) and upward (dashed lines) velocities ($|w| > 0.5$ cm s^{-1}).

3.3.2. Net (longwave) radiative loss

Cooling in thermotopographic flows is associated with net radiative flux divergence (7). However, while net radiation was measured at both 34 and 46 m, the accuracy was not sufficient to give reliable estimates of net radiative flux divergence. Net radiation at a given height, although measured for this study, does not relate directly to heating or cooling. However, negative net radiation indicates that the soil–vegetation–air layer beneath the sensor is losing heat energy, which is likely to lead to cooling air either directly (by radiation divergence) or indirectly (by conduction and convection to vegetation or soil). Moreover, observations show that thermotopographic flows (particularly nocturnal drainage flows) typically occur more frequently in clear sky conditions, when longwave energy is able to escape through the atmospheric window (Barr and Orgill, 1989) allowing the development of a strong surface inversion (Horst and Doran, 1986). Thus, net longwave radiation or outgoing longwave radiation has been used as proxy indicators of radiative flux divergence in some studies of thermotopographic flows (e.g. Barr and Orgill, 1989; Komatsu et al., 2003). Therefore, we compare the nocturnal above-canopy vertical velocities to net radiation measured above the canopy (at 46 or 34 m) during leaf-off and leaf-on periods.

During leaf-off (Fig. 8), there is a slight but consistent positive relation between vertical velocity and net radiation, measured above the leafless forest canopy (the same was found for net radiation below canopy; not shown). There is also a higher probability of downward vertical motion when there is strong net radiative loss. This is consistent with the hypothesis that nocturnal downslope thermotopographic flows may be driving the vertical motion; more net radiative loss results in a stronger temperature inversion, horizontal divergence, and downward vertical flow velocities (vertical convergence).

During leaf-on, there is no clear trend with above-canopy net radiation (34 or 46 m) in the frequency of occurrence of upward or downward motion; however there is a very weak positive relation between mean vertical velocity and net radiation (Fig. 9). This weak relation may or may not indicate that the downward

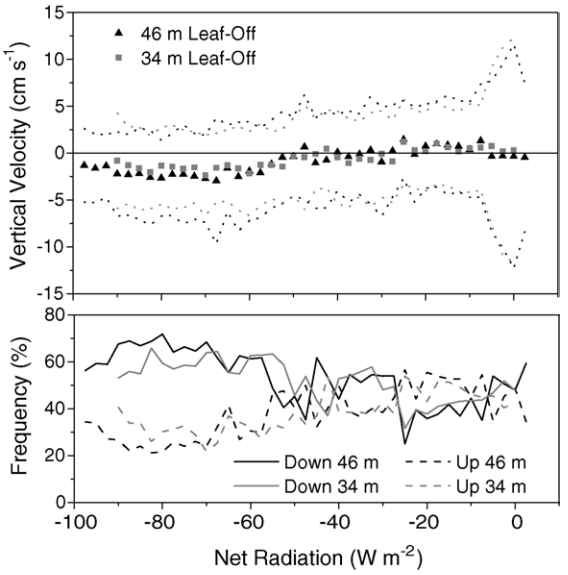

Fig. 8. Nighttime variation of hourly mean vertical velocity with net radiation, during leaf-off seasons (bin-averaged). Upper panel: mean vertical velocity in each bin at 46 (black ▲) and 34 m (gray ■); dotted lines represent ±1 standard deviation from the mean. Lower panel: frequency of occurrence of downward (solid lines) and upward (dashed lines) velocities ($|w| > 0.5\,\mathrm{cm\,s^{-1}}$).

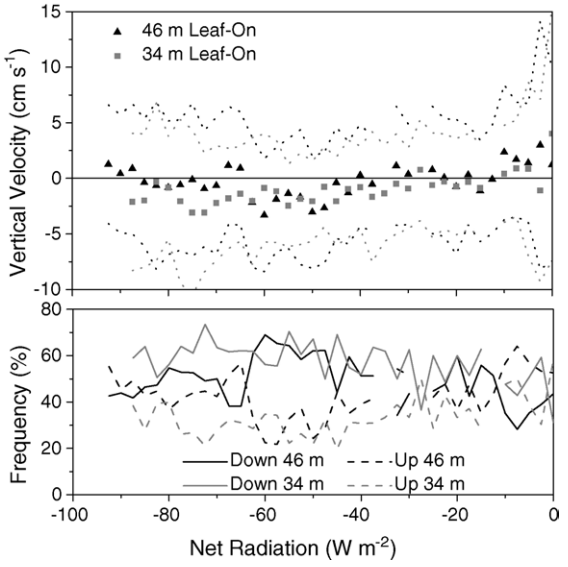

Fig. 9. Nighttime variation of hourly mean vertical velocity with net radiation, during leaf-on seasons (bin-averaged). Upper panel: mean vertical velocity in each bin at 46 (black ▲) and 34 m (gray ■); dotted lines represent ±1 standard deviation from the mean. Lower panel: frequency of occurrence of downward (solid lines) and upward (dashed lines) velocities ($|w| > 0.5\,\mathrm{cm\,s^{-1}}$).

vertical velocities are related to thermally driven flows. At night, there is negative net radiation above the forest canopy; however, radiative divergence and cooling may occur in the canopy, rather than near the ground surface. This radiative loss in the canopy may cause a temperature inversion above the forest canopy, and possibly temperature lapse conditions below the canopy. With the presence of the forest canopy and this possible change in the sign of the temperature gradient above and below the canopy, it is not possible to suggest at what heights (if any) thermotopographic flows may be occurring or to link net radiative loss to possible thermotopographic flows and possible vertical convergence.

While these relations between above-canopy vertical velocity and net radiation are not strong, it is interesting to note the distinct difference between the leaf-on and leaf-off seasons. If vertical flow convergence can be related to radiative cooling in the leaf-off season, it appears that the presence of a closed canopy interferes with this mechanism in a yet to be determined way. Some light is shed on this phenomenon by the study of below-canopy flow and thermal conditions in Froelich and Schmid (2002, 2005).

3.3.3. Stability

An alternative to relating mean vertical velocities to the temperature gradient is to consider the relation with a stability parameter that describes both the strength of a temperature inversion and the horizontal wind shear that generates turbulence and weakens the inversion. Aubinet et al. (2003) and Feigenwinter et al. (2004) each observed upward mean vertical velocities in unstable conditions and downward mean vertical velocities in stable conditions.

Here, we use the bulk Richardson number, R_B (Stull, 1988, p. 177):

$$R_B = \frac{g\Delta\theta_v\Delta z}{\bar{\theta}_v[(\Delta\bar{u})^2 + (\Delta\bar{v})^2]}$$

where, g is the acceleration due to gravity, $\Delta\theta_v$ is the change in virtual potential temperature between two measurement levels separated by height Δz, $\Delta\bar{u}$ and $\Delta\bar{v}$ are changes in the two horizontal components of the mean wind velocity at the two measurement levels, and $\bar{\theta}_v$ is the mean of the temperatures at the measurement levels. We use the bulk Richardson number, rather than the Obukhov length or the flux Richardson number, because these other parameters depend on turbulent fluxes and thus on the method used to determine vertical velocities. Moreover, they are ill-defined when fluxes are small. It is not possible to define an unambiguous threshold to distinguish stable conditions from near-

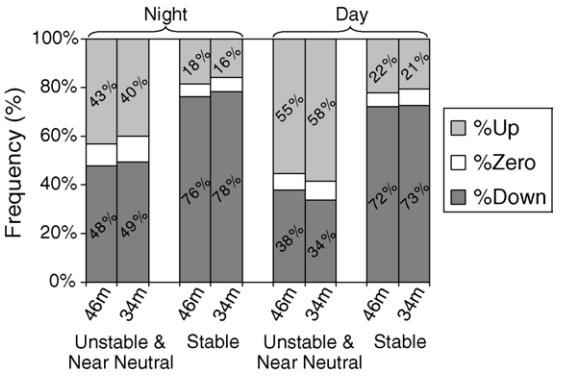

Fig. 10. Frequency of occurrence of downward and upward hourly mean vertical velocities, during stable conditions and during unstable or near-neutral conditions. Stable and unstable or near-neutral are defined as $R_B > 0.1$ and $R_B < 0.1$, respectively. Velocities were considered downward or upward if $|w| > 0.5\,\mathrm{cm\,s^{-1}}$. Number of samples: nighttime unstable or near-neutral 6547; nighttime stable 1892; daytime unstable or near-neutral 8091; daytime stable 267.

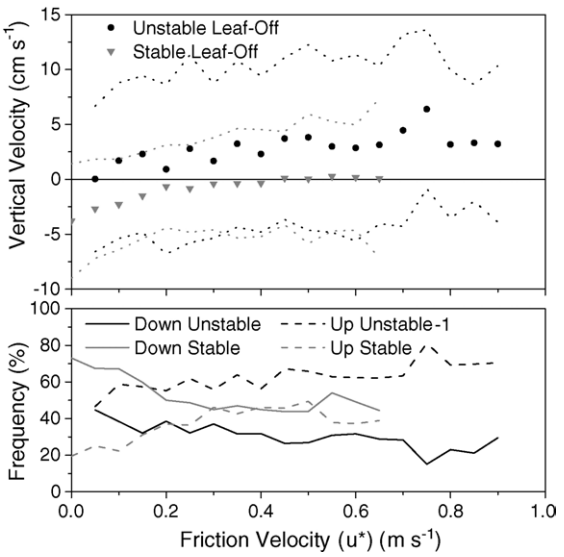

Fig. 11. Leaf-off variation of hourly mean vertical velocity with friction velocity, during stable vs. unstable conditions (bin-averaged) (stable and unstable are defined with respect to the Obukhov length L; stable: $z/L > 0.1$; unstable: $z/L < -0.1$). Upper panel: mean vertical velocity in each bin during unstable (black ●) and stable conditions (gray ▼); dotted lines represent ±1 standard deviation from the mean. Lower panel: frequency of occurrence of downward (solid lines) and upward (dashed lines) velocities ($|w| > 0.5\,\mathrm{cm\,s^{-1}}$).

neutral and unstable; here, we choose to use a value of $R_B = 0.1$ There was a notable change in vertical wind speeds between more stable conditions with higher Richardson numbers ($R_B > 0.1$) and near-neutral to unstable conditions with low Richardson numbers ($R_B < 0.1$) (Fig. 10). From 1999 to 2001, at night, stable conditions occurred 22% of the time, while near-neutral and unstable conditions occurred 78% of the time. In near-neutral to unstable conditions, the vertical velocities had little tendency to either upward or downward motion (46 m vertical velocity was negative in 48% of the cases, positive in 43% of the cases and within 0.005 m s^{-1} of zero in 9% of the cases). In the stable cases, however, there was a strong tendency to downward motion; 46 m vertical velocity was negative in 76% of cases, positive in 18% of cases and near zero in 5% of cases. Similar trends were observed at 34 m, during daytime hours (Fig. 10), and in both leaf-off and leaf-on cases (not shown). This indicates that net downward vertical motion is strongly related to stability.

3.3.4. Friction velocity

Finally, we examine the relation between mean vertical velocity and friction velocity (u^*), in light of the common practice to use u^* as a criterion for rejecting eddy covariance estimates of nighttime (stable condition) fluxes and replacing these with estimates from empirical models of ecosystem exchange. There are two reasons why low u^* may be associated with suspect eddy covariance flux values. Firstly, in stable conditions with low u^* (i.e. low turbulence), turbulent fluxes may be smaller and advection may represent a more significant portion of exchange, than in stable conditions with high u^*. Secondly, in low u^* conditions, shear generated turbulence is less likely to inhibit or weaken thermotopographic flows which may be driving the advection.

During leaf-off, there is a positive relation between vertical velocity and u^* in stable conditions (Fig. 11). The mean vertical velocity is near zero at high values of u^*; downward vertical velocities become stronger and more probable as u^* decreases. The relation is parallel in unstable conditions: the mean vertical velocity is positive for high u^* and decreases as u^* decreases.

During leaf-on (Fig. 12), the relation between vertical velocity and u^* is very similar in both stable and unstable conditions: vertical velocities are more frequently positive for large u^* and become more frequently negative with decreasing u^*.

In both leaf-off and leaf-on, the stable pattern is consistent with the hypothesis that vertical velocities are associated with thermotopographic flows. Higher u^* results in weaker thermotopographic flows and less negative vertical velocities, while in conditions with low u^*, thermotopographic flows are not inhibited by turbulence, and downward motion is stronger. In contrast, for unstable conditions we would expect to see no trend between vertical velocity and u^* based on similar dynamic arguments. However, this is not the

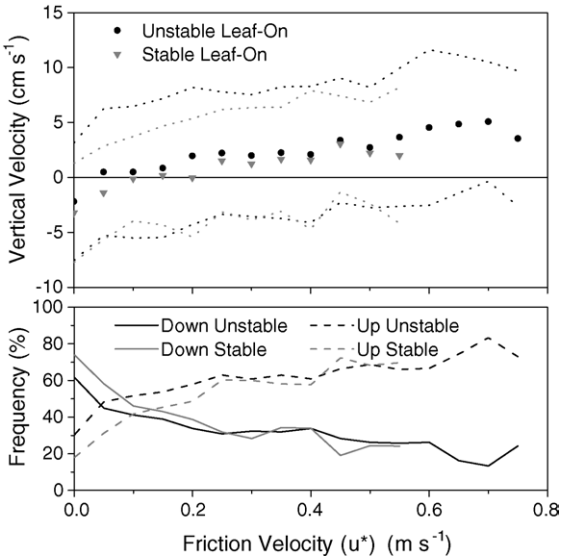

Fig. 12. Leaf-on variation of hourly mean vertical velocity with friction velocity, during stable vs. unstable conditions (bin-averaged) (stable and unstable are defined with respect to the Obukhov length L; stable: $z/L > 0.1$; unstable: $z/L < -0.1$). Upper panel: mean vertical velocity in each bin during unstable (black ●) and stable conditions (gray ▼); dotted lines represent ±1 standard deviation from the mean. Lower panel: frequency of occurrence of downward (solid lines) and upward (dashed lines) velocities ($|w| > 0.5\,\mathrm{cm\,s^{-1}}$).

case. Since the unstable pattern behaves in parallel to the stable one, we cannot reject the possibility that the stable relation is an artifact resulting from the method by which vertical velocities were determined.

4. Conclusions

Mean vertical (i.e. normal-to-slope) motions above the forest canopy at Morgan–Monroe State Forest were determined by rotating measured wind velocities from the sensor coordinate system to a long-term streamline coordinate system, using azimuth-binned averages of vertical rotation angle. These vertical rotation angles were noted to be strongly influenced by local topography. At this site, binned coordinate rotation was preferable to a planar fit method, as the topography is very complex and does not resemble a plane except in very narrow bins.

The vertical velocities tended to be more downward (negative) at night relative to the day. The upward vertical motion is strongest in mid-day. Downward vertical motion is strongest later in the night, consistent with the negative relation observed between vertical velocities and temperature gradients: as temperature gradients tend to increase throughout the night, downward vertical motion also tends to increase. Vertical velocities are generally larger at 46 m than at 34 m, consistent with horizontal divergence (or convergence) in the layer between the two measurement heights.

Vertical velocities were found to be related to temperature gradient, net radiation, and stability. The ensemble relation with these parameters during leaf-off suggests that the vertical convergence at night may be driven by nocturnal thermotopographic flow. A conceptual model of the underlying mechanisms is that consistently strong radiative loss over several hours may lead to a temperature inversion (positive temperature gradient); in conditions when wind shear is not sufficient to support strong turbulent mixing, the temperature inversion may strengthen, leading to density-driven downslope flows. The resulting horizontal divergence at the ridge-top would drive downward vertical motions past eddy-covariance sensors on the tower. The relation between vertical velocities at the two measurement heights indicates that vertical convergence is stronger below 34 m than between 34 and 46 m.

During leaf-on, the relations were more complicated. As during leaf-off periods, nocturnal vertical velocities were negatively correlated to the above-canopy temperature gradient and stability. However, the relations with net radiative loss and friction velocity were less clear. Furthermore, there was evidence that vertical convergence was stronger, on average, at heights between 34 and 46 m than at heights below 34 m. These observations hint at the occurrence of more complex flow patterns during leaf-on. A possible explanation for these relations during leaf-on would be a pattern of vertical convergence above the canopy, driven by strong horizontal flow divergence above the canopy, possibly opposed by horizontal flow convergence below the canopy. Horizontal divergence and convergence are driven respectively by temperature inversions above canopy and lapse conditions below. Stronger evidence to support this possibility is given in Froelich and Schmid (2002, 2005).

The results presented in this paper support the notion that thermotopographic flow is a driver of vertical velocities and vertical convergence, which may be associated with mean scalar transport that is unaccounted for in conventional eddy-covariance measurements. In a companion paper, Froelich and Schmid (2005) examine the occurrences of below canopy thermotopographic flows at MMSF, to further investigate this suggestion.

Acknowledgements

Primary funding for this research was provided by the Biological and Environmental Research Program (BER),

U.S. Department of Energy, through the Midwestern Center of the National Institute for Global Environmental Change (NIGEC) under Cooperative Agreement DE-FC03-90ER61010. Any opinions, findings, and conclusions or recommendations expressed in this publication are those of the authors and do not necessarily reflect the views of the DOE. NJF was supported by a Chancellor's Fellowship from Indiana University. Craig Wayson assisted in our work with the digital terrain model. We gratefully acknowledge the contributions of Steve Scott and the MMSF Field Crew to the operation and maintenance of the MMSF Flux Tower Facility.

References

Amanatidis, G.T., Papadopoulos, K.H., Bartzis, J.G., Helmis, C.G., 1992. Evidence of katabatic flows deduced from a 84 m meteorological tower in Athens, Greece. Bound-Lay. Meteorol. 58, 117–132.

Aubinet, M., Heinesch, B., Yernaux, M., 2003. Horizontal and vertical CO_2 advection in a sloping forest. Bound-Lay. Meteorol. 108, 397–417.

Baldocchi, D., Finnigan, J., Wilson, K., Paw U, K.T., Falge, E., 2000. On measuring net ecosystem carbon exchange over tall vegetation on complex terrain. Bound-Lay. Meteorol. 96, 257–291.

Barr, S., Orgill, M.M., 1989. Influence of external meteorology on nocturnal valley drainage winds. J. Appl. Meteorol. 28, 497–517.

Black, T.A., den Hartog, G., Neumann, H.H., Blanken, P.D., Yang, P.C., Russell, C., Nesic, Z., Lee, X., Chen, S.G., Staebler, R., Novak, M.D., 1996. Annual cycles of water vapour and carbon dioxide fluxes in and above a boreal aspen forest. Glob. Change Biol. 2, 219–229.

Clements, W.E., Archuleta, J.A., Hoard, D.E., 1989. Mean structure of the nocturnal drainage flow in a deep valley. J. Appl. Meteorol. 28, 457–462.

Doran, J.C., Horst, T.W., Whiteman, C.D., 1990. The development and structure of nocturnal slope winds in a simple valley. Bound-Lay. Meteorol. 52, 41–68.

Ehman, J.L., Schmid, H.P., Grimmond, C.S.B., Randolph, J.C., Hanson, P.J., Wayson, C.A., Cropley, F.D., 2002. An initial intercomparison of micrometeorological and ecological inventory estimates of carbon exchange in a mid-latitude deciduous forest. Glob. Change Biol. 8, 575–589.

Feigenwinter, C., Bernhofer, C., Vogt, R., 2004. The influence of advection on the short term CO_2-budget in and above a forest canopy. Bound-Lay. Meteorol. 113, 201–224.

Finnigan, J., 1999. A comment on the paper by Lee (1998): ''On micrometeorological observations of surface-air exchange over tall vegetation''. Agric. Forest Meteorol. 97, 55–64.

Finnigan, J.J., Brunet, Y., 1995. Turbulent airflow in forests on flat and hilly terrain. In: Coutts, M.P., Grace, J. (Eds.), Wind and Trees. Cambridge University Press, Cambridge, pp. 3–40.

Finnigan, J.J., Clement, R., Malhi, Y., Leuning, R., Cleugh, H.A., 2003. A re-evaluation of long-term flux measurement techniques. Part 1: averaging and coordinate rotation. Bound-Lay. Meteorol. 107, 1–48.

Froelich, N.J., Schmid, H.P., 2002. An investigation of advection and gully flows in complex forested terrain. In: 25th Conference on Agricultural and Forest Meteorology. American Meteorological Society, Norfolk VA 10.8.

Froelich, N.J., Schmid, H.P., 2005. Flow divergence and density flows above and below a deciduous forest. Part 2: Below-canopy thermotopographic flows. To be submitted to Agricultural and Forest Meteorology.

Goulden, M.L., Munger, J.W., Fan, S.-M., Daube, B.C., Wofsy, S.C., 1996. Measurements of carbon sequestration by long-term eddy covariance: methods and a critical evaluation of accuracy. Glob. Change Biol. 2, 169–182.

Horst, T.W., Doran, J.C., 1986. Nocturnal drainage flow on simple slopes. Bound-Lay. Meteorol. 34, 263–286.

Jarvis, P.G., Massheder, J.M., Hale, S.E., Moncrieff, J.B., Rayment, M., Scott, S.L., 1997. Seasonal variation of carbon dioxide, water vapor, and energy exchanges of a boreal black spruce forest. J. Geophys. Res. 102 (D), 28,953–28,966.

Komatsu, H., Yoshida, N., Takizawa, H., Kosaka, I., Tantasirin, C., Suzuki, M., 2003. Seasonal trend in the occurrence of nocturnal drainage flow on a forested slope under a tropical monsoon climate. Bound-Lay. Meteorol. 106 (3), 573–592.

Lee, X., 1998. On micrometeorological observations of surface-air exchange over tall vegetation. Agric. Forest Meteorol. 91, 39–49.

Lee, X., Hu, X., 2002. Forest-air fluxes of carbon, water and energy over non-flat terrain. Bound-Lay. Meteorol. 103, 277–301.

Mark, D.M., Church, M., 1977. On the misuse of regression in earth science. Math. Geol. 9 (1), 63–75.

McMillen, R.T., 1988. An eddy correlation technique with extended applicability to non-simple terrain. Bound-Lay. Meteorol. 43, 231–245.

Paw U, K.T., Baldocchi, D.D., Meyers, T.P., Wilson, K.B., 2000. Correction of eddy-covariance measurements incorporating both advective effects and density fluxes. Bound-Lay. Meteorol. 97, 487–511.

Sakiyama, S.K., 1990. Drainage flow characteristics and inversion breakup in two Alberta mountain valleys. J. Appl. Meteorol. 29, 1015–1030.

Schmid, H.P., Grimmond, C.S.B., Cropley, F., Offerle, B., Su, H.-B., 2000. Measurements of CO_2 and energy fluxes over a mixed hardwood forest in the mid-western United States. Agric. Forest Meteorol. 103, 357–374.

Smith, M.O., Simpson, J.R., Fritschen, L.J., 1985. Spatial and temporal variation of eddy flux measures of heat and momentum in the roughness sub-layer above a 30 m Douglas-fir forest. In: Hutchison, B.A., Hicks, B.B. (Eds.), The Forest-Atmosphere Interaction. D. Reidel Publishing Company, Dordrecht, pp. 563–581.

Stull, R.B., 1988. An Introduction to Boundary Layer Meteorology. Kluwer Academic Publishers, Dordrecht, pp. 670.

Su, H.-B., Schmid, H.P., Grimmond, C.S.B., Vogel, C.S., Curtis, P.S., 2000. Temporal and spatial variability of mean flow and turbulence characteristics over a deciduous forest. In: Preprints: 14th Symposium on Boundary Layers and Turbulence. American Meteorological Society, Aspen CO P6C.3.

Su, H.-B., Schmid, H.P., Grimmond, C.S.B., Vogel, C.S., Oliphant, A.J., 2004. Spectral characteristics and correction of long-term eddy-covariance measurements over two mixed hardwood forests in non-flat terrain. Bound-Lay. Meteorol. 110, 213–253.

Whiteman, C.D., 1990. Observations of thermally developed wind systems in mountainous terrain. In: Blumen, W. (Ed.), Atmospheric Processes over Complex Terrain. American Meteorological Society, Boston, MA, pp. 5–42.

Wilczak, J.M., Oncley, S.P., Stage, S.A., 2001. Sonic anemometer tilt correction algorithms. Bound-Lay. Meteorol. 99, 127–150.

Wofsy, S.C., Goulden, M.L., Munger, J.W., Fan, S.-M., Bakwin, P.S., Daube, B.C., Bassow, S.L., Bazzaz, F.A., 1993. Net exchange of CO_2 in a mid-latitude forest. Science 260, 1314–1317.